RESEARCH LETTER

Key Points:
- Organic carbon export efficiency is inversely related to primary production
- Zooplankton faecal pellets control transfer efficiency in the Southern Ocean
- Zooplankton vertical migration fluxes transfers high quality material to depth

Supporting Information:
- Table S1
- Figure S1

Correspondence to:
E. L. Cavan,
e.cavan@noc.soton.ac.uk

Attenuation of particulate organic carbon flux in the Scotia Sea, Southern Ocean, is controlled by zooplankton fecal pellets

E. L. Cavan[1], F. A. C. Le Moigne[2,3], A. J. Poulton[2], G. A. Tarling[4], P. Ward[4], C. J. Daniels[1], G. M. Fragoso[1], and R. J. Sanders[2]

[1]National Oceanography Centre, University of Southampton, Southampton, UK, [2]National Oceanography Centre, Southampton, UK, [3]Now at GEOMAR Helmholtz Centre for Ocean Research Kiel, Kiel, Germany, [4]British Antarctic Survey, Cambridge, UK

Abstract The Southern Ocean (SO) is an important CO_2 reservoir, some of which enters via the production, sinking, and remineralization of organic matter. Recent work suggests that the fraction of production that sinks is inversely related to production in the SO, a suggestion that we confirm from 20 stations in the Scotia Sea. The efficiency with which exported material is transferred to depth (transfer efficiency) is believed to be low in high-latitude systems. However, our estimates of transfer efficiency are bimodal, with stations in the seasonal ice zone showing intense losses and others displaying increases in flux with depth. Zooplankton fecal pellets dominated the organic carbon flux and at stations with transfer efficiency >100% fecal pellets were brown, indicative of fresh phytodetritus. We suggest that active flux mediated by zooplankton vertical migration and the presence of sea ice regulates the transfer of organic carbon into the oceans interior in the Southern Ocean.

1. Introduction

The biological carbon pump (BCP) transfers carbon from the surface to the deep ocean [*Eppley and Peterson*, 1979] via the sinking of organic carbon produced in the surface. Up to 40% of primary production is exported out of the mixed layer [*Henson et al.*, 2011] via sinking and the active transport of metabolites and unassimilated waste by zooplankton diel vertical migration (DVM) [*Herndl and Reinthaler*, 2013]. Remineralization of particulate organic carbon (POC) to CO_2 by bacteria and zooplankton means that only a small fraction of this flux reaches the interior with the depth distribution of remineralization controlling atmospheric CO_2 levels [*Kwon et al.*, 2009].

The Southern Ocean (SO) accounts for ~20% of the global ocean CO_2 uptake [*Takahashi et al.*, 2002; *Park et al.*, 2010], with biological processes being responsible for seasonal variations in air-sea flux of CO_2. The SO is a large high-nutrient-low-chlorophyll region, likely due to limited iron availability [*Martin*, 1990]. Nevertheless, iron from oceanic islands and melting sea ice can cause intense phytoplankton blooms, which may lead to high POC export [*Pollard et al.*, 2009].

It is uncertain what factors control the fraction of production that is exported (particle export efficiency (PEeff)) and how efficiently this material is transferred to depth (transfer efficiency (Teff)) on both global and regional scales. *Laws et al.* [2000] showed a global positive, linear relationship between PEeff and primary production. More recently, *Maiti et al.* [2013] observed a negative relationship in the SO, suggesting that high export occurs during periods of low primary production. Further work based on a global examination of ballast content of surface sinking material suggested that Southern Ocean (SO) ecosystem processes may have a greater importance than ballast content in driving PEeff and Teff [*Le Moigne et al.*, 2014].

Francois et al. [2002] and *Le Moigne et al.* [2012] suggest that mineral ballasting is a potential controller of Teff, although the degree of recycling in the mesopelagic zone [*Henson et al.*, 2012] and epipelagic ecosystem structure [*Lam et al.*, 2011] are thought to be important. Regardless of the dominant control, these studies suggest that low Teff occurs in productive, high-latitude regions where opal-producing organisms dominate the phytoplankton community. In contrast, *Buesseler et al.* [2007] observed high Teff at high latitude (K2, north Pacific), although this was using neutrally buoyant sediment traps over different depth horizons compared to the previous studies.
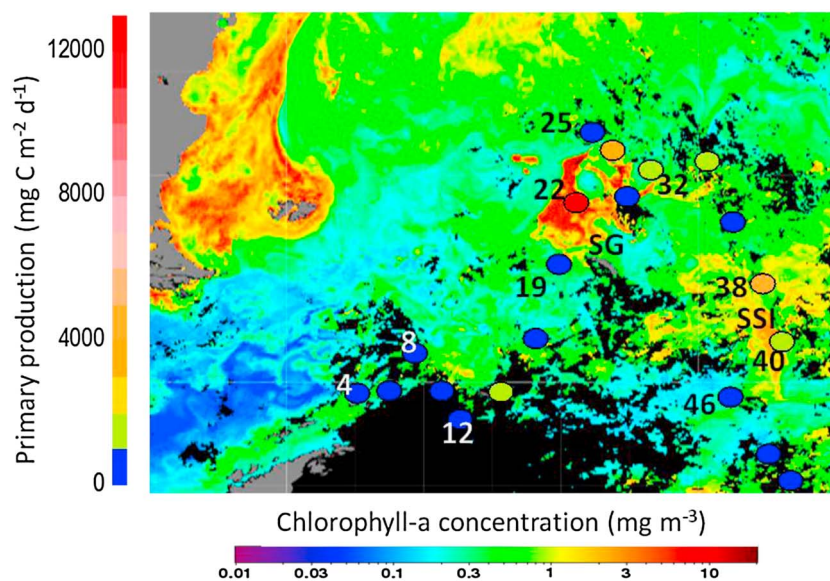
Figure 1. Satellite chlorophyll *a* image (Aqua Moderate Resolution Imaging Spectroradiometer from oceancolor.gsfc.nasa. gov, monthly composite for January 2013) with in situ primary production rates. The numbers represent station numbers. SG = South Georgia. SSI = South Sandwich Islands. Black represents cloud and sea ice cover. The continuous black coverage below station 12 is due to sea ice.

To understand the variability in flux attenuation in high-latitude waters and the potential controls over the transfer of POC to depth in the Southern Ocean, we deployed marine snow catchers (MSCs) in the Scotia Sea, where POC export estimates are scarce [*Le Moigne et al.*, 2013]. We calculated POC flux in the upper mesopelagic zone at sites with varying levels of primary production and then calculated PEeff and Teff. To quantify Teff, we used Martin's *b* (F_b, the attenuation coefficient in the power function described by *Martin et al.* [1987]). A high positive F_b describes a large attenuation of POC with depth, therefore, high remineralization of POC in the mesopelagic. The average F_b calculated by *Martin et al.* [1987] from the North Pacific was 0.86. Recent analyses suggest that F_b ranges between 0.2 and 4 globally and in the SO from 0.9 to 3.9 [*Francois et al.*, 2002; *Lam and Bishop*, 2007; *Henson et al.*, 2012]; thus, the SO is a region of high mesopelagic remineralization and low Teff. Our aims were to (1) test the hypothesis that PEeff is negatively related to primary production, (2) estimate F_b in situ in the SO, and (3) identify what controls F_b.

2. Methods

Observations were made in the Scotia Sea (Figure 1) during RRS *James Clark Ross* cruise JR274 (11 January to 5 February 2013). Samples for chlorophyll *a* (chl *a*), biogenic silica, and primary production were taken using Niskin bottles mounted on a conductivity-temperature-depth rosette sampler. Bongo nets to determine zooplankton abundance were deployed between 0 and 200 m at approximately 05:00 UT and 17:30 UT with samples being immediately preserved [*Ward et al.*, 2005]. The MSCs were deployed to 10 m and 110 m below the mixed layer depth (MLD) (henceforth referred to as MLD + 10 m and MLD + 110 m, respectively). The MLD ranged from 20 to 70 m, and all deployments occurred around 06:00 local time.

2.1. Phytoplankton Composition and Production

Chl *a* was measured by filtering seawater (0.2 L) through a glass fiber filter or 2, 5, 10, or 20 μm membrane filters. Chl *a* was extracted in 90% acetone overnight and fluorescence quantified using a fluorometer (Turner Trilogy) calibrated with a solid standard and chl *a* extract. Biogenic silica concentration was measured by filtering 1 L of seawater through a 10 μm membrane filter, digesting it with sodium hydroxide, neutralizing with hydrochloric acid, and measuring the silicate concentration using an autoanalyzer [*Brown et al.*, 2003]. Daily rates of primary production were measured following *Poulton et al.* [2014]. Water samples (70 mL, 3 light, 1 formalin killed) from the middle of the mixed layer were inoculated with 28–30 μCi of ^{14}C-labeled sodium bicarbonate and either incubated for 24 h in chilled surface seawater with the light depth replicated

using Misty-blue optical filters (LEE™) or in a refrigeration container [*Richier et al.*, 2014]. The average relative standard deviation of triplicate (light) measurements was 20% (2–51%).

2.2. Zooplankton

Samples were collected using a motion-compensated bongo net system equipped with 200 μm mesh nets with 0.61 m diameter mouth openings [*Ward et al.*, 2012a]. The whole samples were examined, and moderately abundant, large, and /or rare taxa were enumerated. The sample was then split using a Folsom plankton splitter to provide total counts of ~100–200 of the larger organisms (1/2–1/64) and 1–2 further splits for the smaller organisms (1/32–1/512), resulting in around 500–750 individual organisms per sample. Data from splits were standardized to per catch and then to ind m^{-2} using a calculation of mouth area multiplied by the vertical sampling interval (200 m). No flowmeters were used on the net as the slow hauling speed employed is at the bottom end of the calibration range for most flowmeters. We assumed 100% sampling efficiency as no obvious clogging of the nets occurred.

2.3. Particulate Organic Carbon Flux

Marine snow catchers are large (95 L) water bottles used as settling columns [see *Riley et al.*, 2012]. After recovery, they stood for 2 h, allowing the particles to settle. Visible particles were picked from the base using a Pasteur pipette and classified under a microscope (Olympus SZX16) as either phytodetrital aggregates (PDAs) or fecal pellets (FPs). Photographs (Canon T2-EOS) of the particles were taken to estimate size, volume, and POC content. SigmaScan Pro 4 was used to determine the equivalent spherical diameter of PDAs, but for FPs, the diameter and length were measured from photographs to calculate volume. Conversion factors from *Alldredge* [1998] were used to estimate the POC mass following equations (1) and (2):

$$PDA\ POC(\mu g) = 1.09 \times v^{0.52} \tag{1}$$

$$FP\ POC(\mu g) = 1.05 \times v^{0.51} \tag{2}$$

where v is the estimated volume of the particle in cubic millimeters.

Particle sinking rates were measured using a glass measuring cylinder filled with seawater at in situ temperature [*Riley et al.*, 2012]. The time for particles to pass two marked points (halfway down the 1 L cylinder) was timed. Sinking fluxes were calculated following *Riley et al.* [2012], where flux (mgC m^{-2} d^{-1}) is the mass of POC divided by the surface area of the base of the MSC (0.06 m^{-2}) and the sinking time of particles (days), scaled up to the time to sink the length of the marine snow catcher:

$$Sinking\ time(d) = \frac{1}{w} \tag{3}$$

where l is the length of the marine snow catcher (1.5 m) and w is the measured sinking rate from the sinking experiments.

3. Results and Discussion

3.1. Phytoplankton Production Patterns

The cruise crossed the mean position of the Polar Front and the southern boundary of the Antarctic Circumpolar Current (Figure 2a). Stations south of 60°S were in the seasonal ice zone (SIZ), and one station (12, >15% ice cover) was in the marginal ice zone (MIZ) [*Tarling*, 2013]. Peak total chl a concentrations were observed northwest of South Georgia (17 μg L^{-1}) and north of the South Sandwich Islands (11 μg L^{-1}) (Figure 2b). These areas had both high (16 and 10 μg L^{-1}, respectively) concentrations of chl a >20 μm (Figure S1d in the supporting information) and biogenic silica suggesting high concentrations of diatoms in these regions (Figure 2d).

Primary production showed a similar distribution to chl a (Pearson's product-moment correlation, $r^2 = 0.96$, $p < 0.001$, $n = 18$), with values >12 gC m^{-2} d^{-1} northwest of South Georgia and >4.5 gC m^{-2} d^{-1} north of the South Sandwich Islands (Figure 1). The general distribution and magnitude of chl a and primary production match well with previous studies in the Scotia Sea [e.g., *Korb et al.*, 2012].
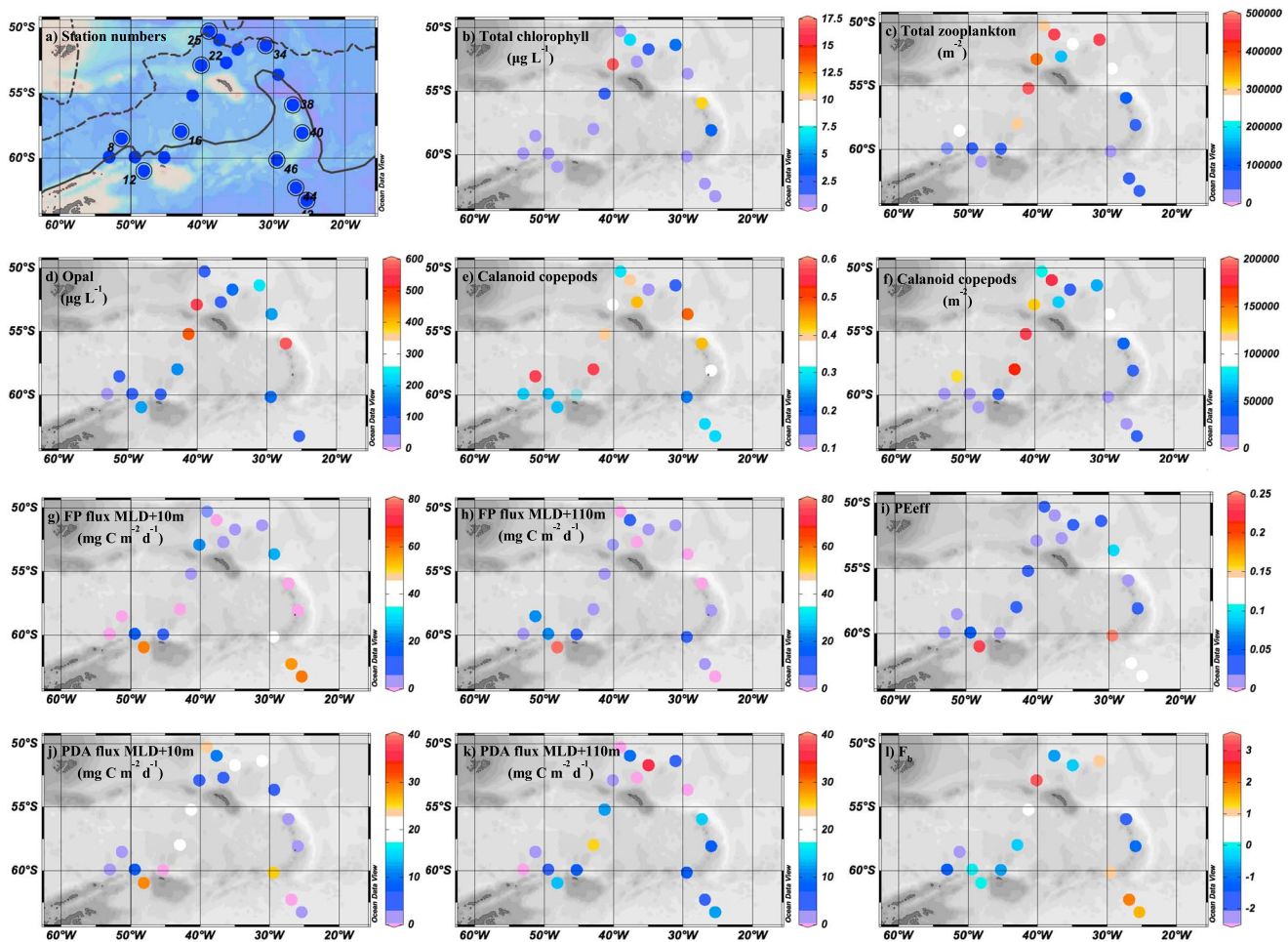
Figure 2. Maps of (a) stations: mean polar front position (dashed line) and southern boundary of the Antarctic circumpolar current (solid line), (b) total chlorophyll *a*, (c) zooplankton abundance (excluding euphausiids), (d) opal concentration, (e) proportion of calanoids, (f) calanoid copepod abundance, (g and h) FP flux at MLD + 10 m (Figure 2g) and MLD + 110 m (Figure 2h), (i) export efficiency (PEeff), (j and k) PDA flux at MLD + 10 m (Figure 2j) and MLD + 110 m (Figure 2k), and (l) POC attenuation (F_b).

3.2. Zooplankton Abundance

Catches were numerically dominated by cyclopoid copepods, which may have a role in the degradation and remineralization of fecal pellets [*González and Smetacek*, 1994; *Iversen and Poulsen*, 2007]. Calanoid copepods were the next most abundant taxa (Figure 2f) including many species known to graze on phytoplankton and to perform DVM [*Atkinson et al.*, 1992]. Euphausiids were present in the study region, but net avoidance meant that no quantitative data on their abundance is available. Total zooplankton and calanoid copepod levels were low ($<15{,}000$ ind m^{-2} and <5000 ind m^{-2}, respectively) in the SIZ and at the South Sandwich Islands, where chl *a* was relatively high. Zooplankton abundance was ~5 times higher around South Georgia and in the open ocean, where chl *a* was low (Figure 2e). Mismatches between phytoplankton and zooplankton abundance may be due to the dynamics of sea ice retreat in this region [*Clarke and Peck*, 1991] and /or the seasonal vertical migrations of late-stage copepodites ascending into surface waters after spending the preceding winter at depth [*Tarling et al.*, 2004].

3.3. Exported Particulate Organic Carbon

The mean mass (± standard deviation, calculated using *Alldredge*'s [1998] equations) of sinking POC in the entire 95 L MSC was 7 ± 0.13 μg at MLD + 10 m and 3.5 ± 0.15 μg at MLD + 110 m. The mean particle sinking rates ranged from 50 to 430 ± 42 m d^{-1} (standard deviation) (Table S1 in the supporting information). There was no significant difference ($p > 0.05$, Student's *t* test) between the sinking rates or abundance of FPs and PDAs.
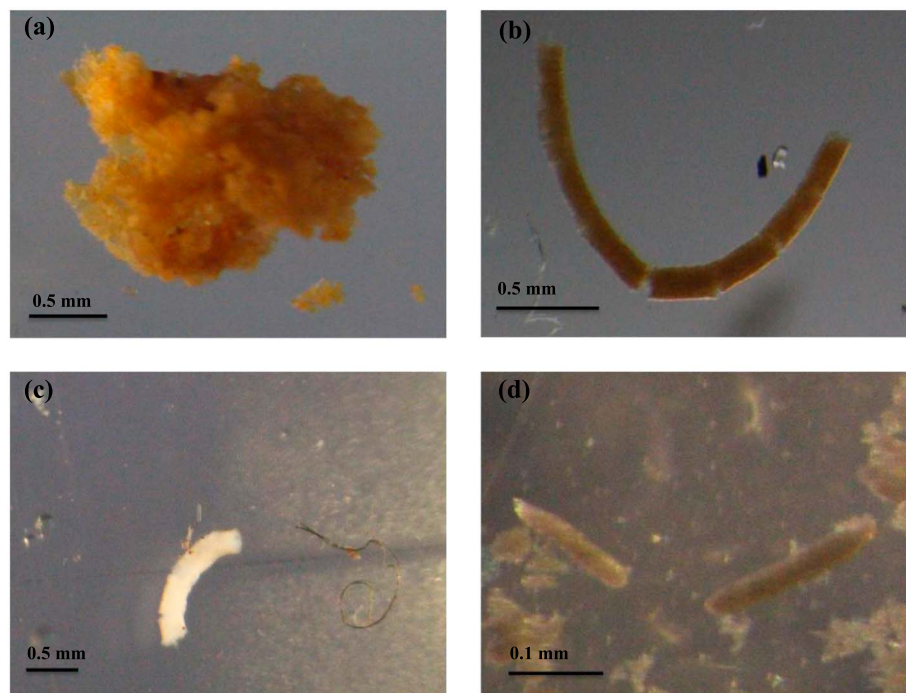
Figure 3. Photographs of particles: (a) PDA, (b) brown krill FP, (c) white FP, and (d) copepod FP.

POC flux ranged from 0 to 91 mgC m^{-2} d^{-1}. FP flux ranged between 0 and 78 mgC m^{-2} d^{-1}, with a maximum observed in the marginal ice zone at MLD + 110 m (Figures 2g and 2h). The PDA flux was much smaller, only ranging from 0 to 36 mgC m^{-2} d^{-1} (Figures 2j and 2k). The FP flux was strongly correlated (Pearson's product-moment correlation) with the total mass at both depths (MLD + 10 m, $r^2 = 0.92$, $p < 0.001$, $n = 19$; MLD + 110 m, $r^2 = 0.90$, $p < 0.001$, $n = 19$). However, correlations between PDA flux and mass, although significant ($p < 0.05$), were not as strong (MLD + 10 m, $r^2 = 0.48$, $n = 19$; MLD + 110 m, $r^2 = 0.49$, $n = 19$) highlighting that FPs drove much of the variability in POC flux. The proportion of total POC flux due to FPs was 66–100% in the SIZ and 0–68% at South Georgia and the South Sandwich Islands.

High FP export was observed in the SIZ (stations 43–46) and the MIZ at MLD + 10 m (Figure 2g) even though total zooplankton abundance was low in this region. Antarctic krill (*Euphausia superba*) were most likely to be responsible for this high FP export as throughout the sampling region, 82% of the FPs were of euphausiid origin, the remainder being recognizable copepod pellets (Figures 3b–3d). There was an increase in FP flux at MLD + 110 m relative to MLD + 10 m in the MIZ, whereas in the SIZ, there was a large decrease in FP flux with depth. This pattern was not reflected in the PDA flux.

The MSC-derived estimates of POC flux are consistent with other measurements in the region; for example, *Ducklow et al.* [2008] measured fluxes of 12–120 mgC m^{-2} d^{-1} using moored sediment traps at the Western Antarctic Peninsula, while *Planchon et al.* [2013] calculated fluxes of 11–61 mgC m^{-2} d^{-1} using the Th-234 method in the Atlantic Southern Ocean, and finally, *Salter et al.* [2007] measured fluxes of 28–46 mgC m^{-2} d^{-1} using the drifting sediment trap Particle Export measurement using LAGRAngian sediment traps (PELAGRA) at the Crozet Plateau. The comparability of MSC fluxes to those from other approaches indicates that the MSC is a robust method for estimating POC flux.

3.4. Export From the Mixed Layer

The highest values of PEeff were observed in the SIZ (25%, Figure 2i) rather than in the highly productive, opal-dominated blooms (Figure 2d), which are often thought to be hot spots of carbon export in the SO [*Korb et al.*, 2012]. This suggests that diatoms were not directly important for export flux, but they may have been important indirectly following consumption by zooplankton and the subsequent production of zooplankton FPs.
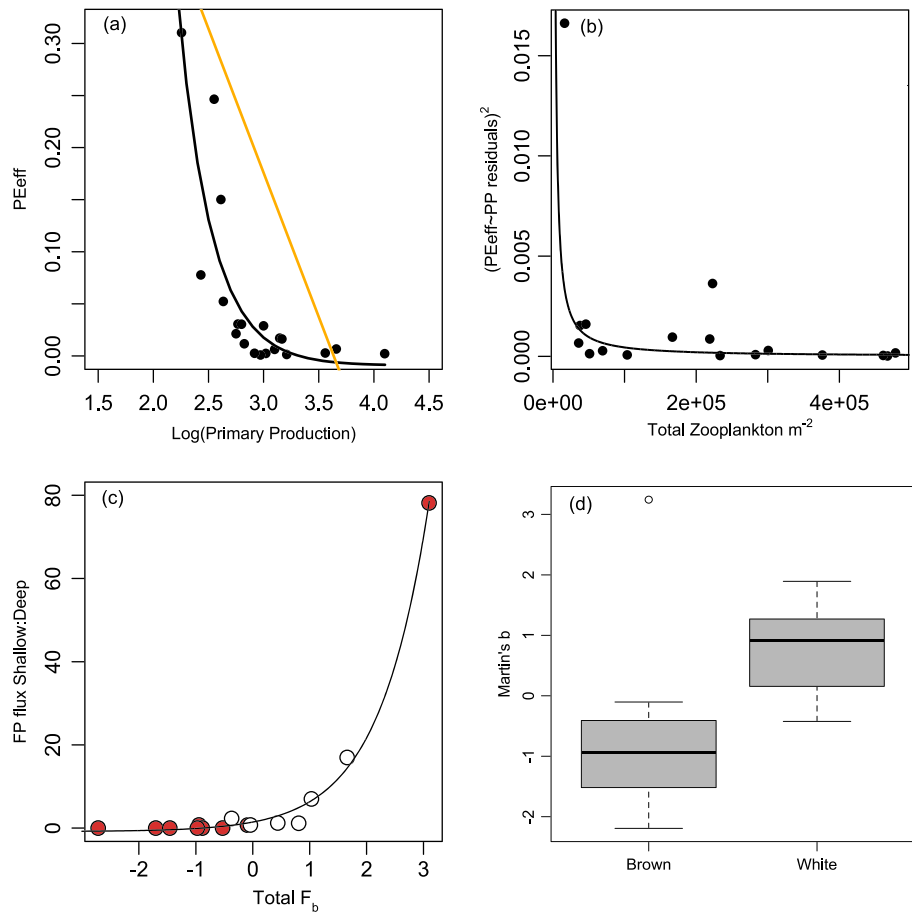
Figure 4. (a) PEeff against log (primary production) (mgC m^{-2} d^{-1}), orange line from *Maiti et al.* [2013]; the black line is the nonlinear regression (equation (4)). (b) Total zooplankton abundance against the square of the residuals from Figure 4a (equation (5)). (c) Ratio of shallow to deep FP flux against F_b (the color indicates dominant color of fecal pellets; the black line is the nonlinear regression (equation (6)). (d) Average (solid black lines) and standard deviations of F_b for different colored fecal pellets.

Previously, higher (<30%) values of PEeff were measured off the western Antarctic Peninsula by *Buesseler et al.* [2010]. PEeff reached a maximum of 25% in this study (Figure 2i), which is closer to the maximum values reported by *Henson et al.* [2012]. However, the mean value across the study region was much lower at 5.1% (±0.42 standard deviation) due to a range of 0–30%, similar to that calculated by *Planchon et al.* [2013].

Previous work has revealed a positive linear relationship between primary production and PEeff [*Laws et al.*, 2000]. Our data instead shows that an inverse relationship between primary production and PEeff was observed (Figure 4a), a pattern also recently reported by *Maiti et al.* [2013] in the SO. *Maiti et al.* [2013] observed a linear relationship between primary production and PEeff; however, in our study, a nonlinear regression (equation (4)) best fits the data ($r^2 = 0.75$, $p < 0.01$, $n = 18$; Figure 4a).

$$\text{PEe}ff = 538 \times e^{(-3.3 \times \text{LogPP})} \tag{4}$$

An inverse relationship between PEeff and primary production means that a high fraction of primary production is exported when primary production is low. This could be due to temporal decoupling between primary production and export [*Salter et al.*, 2007], which may account for <60% of the variability in the relationship between PEeff and primary production [*Henson et al.*, 2014]. Alternatively, seasonal dynamics of the zooplankton community may explain this variation. For instance, many calanoid copepods overwinter at depth and arrive in the surface layers in advance of the bloom [*Tarling et al.*, 2004], and the same may also apply to Antarctic krill [*Kawaguchi et al.*, 1986]. Discarded moults, natural mortality, and predation mortality from this

overwintering community will enhance POC levels independently of the timing of phytoplankton blooms. Alternatively, *Maiti et al.* [2013] suggested that processes like zooplankton grazing, heavy remineralization, and a large export of dissolved organic carbon were responsible for this relationship.

Zooplankton grazing could be a significant factor due to the varying stability of phytoplankton growth in the SO. Primary production in the SIZ is stable, whereas further north in the open water seasonal variation is large. Here steep primary production gradients exist, which are caused by the influence of eddy-mediated cross frontal mixing, transporting nutrients and increasing chl *a* [*Kahru et al.*, 2007; *Dulaiova et al.*, 2009]. Thus, zooplankton grazers can develop and graze down phytoplankton in the SIZ, whereas in the open water, the grazers do not develop quickly enough in response to a bloom to have a significant effect on primary production (Figure 4a). Therefore, we assessed if the presence of zooplankton could further explain this relationship by calculating the residuals (Residuals^2) between the best fit line and the data points in Figure 4a and comparing them with zooplankton abundance (*Z*). We found that zooplankton abundance (equation (5) and Figure 4b) explained 40% ($p < 0.01$) of the variance between primary productivity and PEeff.

$$\text{Residuals}^2 = 5.0 \times Z^{-1.1} \tag{5}$$

Thus, although grazing probably does not dictate the overall shape of the relationship between PEeff and primary production, here we show for the first time clear evidence of its capacity to modulate this relationship and the importance of zooplankton in transferring organic carbon from the surface to the interior Southern Ocean.

3.5. POC Transfer Through the Upper Mesopelagic Zone

Once exported from the mixed layer, POC sinks into the ocean's interior where it is utilized by bacteria and zooplankton, reducing the size of the sinking flux with depth [*Martin et al.*, 1987; *Steinberg et al.*, 2008; *Giering et al.*, 2014]. We fitted the power function of *Martin et al.* [1987] (F_b) to the data to quantify the decrease in POC flux with depth. At 47% of the stations, POC flux decreased with depth, resulting in positive F_b values, whereas the remaining stations showed an increase in POC flux with depth, leading to negative F_b values. Overall, F_b ranged from -2 to 3 with a mean of 0 (± 1.4) (Figure 2l). This implies an overall negligible attenuation of POC flux in the upper mesopelagic of the Scotia Sea, with the mean Teff being almost 100%. Negative F_b values and increasing POC flux with depth may be due to lateral advection at depth, flux integration time scales, or zooplankton DVM. Lateral advection is unlikely to have driven the observed increased fluxes at depth, as MSC deployments were <175 m and therefore all within the single water mass classified as surface water by *Heywood and King* [2002], which occurs <200 m between 45 and 65°S. Additionally, as FPs dominated the flux (see section 3.3), any pulse of flux in phytoplankton such as diatoms, which can occur in the SO [*Salter et al.*, 2012], would have had a limited effect on F_b. Therefore, we assume that our interpretation of fluxes is correct, and possible controls of F_b, including DVM, are discussed in the following section.

3.6. Controls Over Mesopelagic Flux Attenuation

Mesopelagic POC Teff is a key metric of the BCP [*Buesseler and Boyd*, 2009] and is linked to the amount of CO_2 stored in the interior by biological processes [*Kwon et al.*, 2009]. There was no significant effect of primary production on F_b (Pearson's product-moment correlation, $p > 0.05$, $n = 15$), suggesting that production is unlikely to control variability in mesopelagic remineralization. Given that flux was dominated by FPs (Figures 2g and 2h) and the distribution of transfer efficiencies is linked to sea ice (a major distinguishing factor for ecosystems in the SO [*Ward et al.*, 2012b; *Murphy et al.*, 2013]), we initially test the hypotheses that zooplankton processes are involved and that these may change with sea ice cover. Sea ice retreat increases the vertical stability of the water column so phytoplankton can remain in the water column longer [*Taylor et al.*, 2013], and a pulse of flux often occurs after sea ice retreat [*Ducklow et al.*, 2008].

We calculated the ratios of shallow FP flux to deep FP flux (the FP flux ratio) and plotted these against F_b (Figure 4c). The change in FP flux ratio is significantly related to the attenuation of POC (quantified as F_b) via an exponential regression ($r^2 = 1$, $p < 0.001$):

$$\text{FP flux ratio} = -0.83 + 2.28 \times e^{(1.1 \times F_b)} \tag{6}$$

No significant relationship exists between a similarly calculated PDA flux ratio and POC attenuation (F_b), again highlighting the important role of zooplankton in controlling the transfer of POC to depth in the Southern Ocean.

Zooplankton can cause depth variability in flux via the active transfer of organic carbon due to DVM [*Wilson et al.*, 2008]. Zooplankton consume organic matter in the surface layer and then descend prior to releasing a fraction of it through respiration, excretion, and defecation. Such DVM behavior is well documented in our study area; for example, *Atkinson et al.* [1992] identified four copepod species near South Georgia migrating from a daytime depth of up to 120 m (55 m above the deepest MSCs) to the surface layers at night. Similar effects of DVM on flux profiles have been postulated in the Arabian Sea [*Wishner et al.*, 2008].

The presence of sea ice may influence the extent to which DVM and active flux occur. The mixed layer depth was between 20 m and 30 m in the sea ice zone compared to >40 m in regions farther from the sea ice (S. Thorpe, JR274 physical oceanographic analyses, British Antarctic Survey, unpublished report, 2014, http://nora.nerc.ac. uk/id/eprint/508783). The reduction of the upper mixed layer depth in the SIZ would mean that even zooplankton with less extensive DVMs are more likely to contribute to active flux than in "deep" mixed layer depth conditions. Moreover, the level of active flux is enhanced by the reduced time required to migrate out the mixed layer. Sea ice will also have an effect on light levels as ice lowers the penetration of downwelling irradiance into the ocean (typically between 15% and 90% [*Grenfell and Maykut*, 1977]) through an increase in surface albedo and absorption. The response to lowered light levels may be species specific; krill may reduce their DVM in the presence of ice as it protects them from their visual predators such as fur seals and macaroni penguins [*Veit et al.*, 1993]; however, copepods may not as their predators, such as larval fish and chaetognaths [*Froneman et al.*, 1998; *Turner*, 2004], are less effected by ice. However, in the MIZ, FP flux increased with depth, suggesting the presence of DVM, but in the SIZ, FP flux decreased (Figure 1 and Figures 2g and 2h), and these ice zones are likely dominated by krill, whereas copepods dominate in open water areas [*Siegel et al.*, 1992]. *Lancroft et al.* [1991] also observed DVM by krill in the ice-covered Scotia Sea.

Taken together, the presence of sea ice and DVM can explain the broad geographical patterns of change in POC flux with depth. However, there are exceptions to these patterns, and we hypothesize that diet may strongly link to the size of the active flux. White FPs indicate feeding on detritus, FPs, or transparent flagellates, whereas brown FPs indicate feeding on fresh phytoplankton [*Wilson et al.*, 2008]. Data points on Figure 4c are colored white or brown, indicating the dominant (>70% abundance) color of FPs at each station. Where F_b was positive, most of the FPs were white, and where it was negative, most pellets were brown. The effect of the color of pellet on F_b was statistically significant (one-way analysis of variance, $F = 21.26$, $df = 13$, $p < 0.001$; Figure 4c; note that station 22 was an anomaly, where $F_b > 3$). The deviation to this rule was station 12 in the MIZ. This suggests that active transport is most pronounced where zooplankton were exclusively feeding on fresh phytoplankton, with zooplankton consuming detrital material in environments where the active flux and hence Teff are low.

4. Summary

Export efficiency in the Scotia Sea was inversely related to primary production, supporting the observations of *Maiti et al.* [2013]. Further, we suggest that zooplankton processes are an important contributor to this relationship. The efficiency with which this exported material is transferred to the interior regulates the role ocean biological processes play in controlling atmospheric CO_2 levels. We find that the upper mesopelagic element of this transfer is highly variable in the Scotia Sea, with zooplankton fecal pellets dominating flux. Active transport via surface ingestion and deep defecation linked to diel vertical migration is a key process involved in transferring material out of the euphotic zone, which appears to operate most strongly when zooplankton graze on fresh organic material and sea ice is present. Climate change may reduce zooplankton abundance and change community structure [*Atkinson et al.*, 2004]; any associated reduction in FP production will reduce the depth penetration of organic carbon, with long-term implications for atmospheric CO_2 and the SO carbon cycle.

References

Alldredge, A. (1998), The carbon, nitrogen, and mass content of marine snow as a function of aggregate size, *Deep Sea Res., Part I*, *45*(4–5), 529–541, doi:10.1016/S0967-0637(97)00048-4.

Atkinson, A., P. Ward, R. Williams, and S. Poulet (1992), Feeding rates and diel vertical migration of copepods near South Georgia: Comparison of shelf and oceanic sites, *Mar. Biol.*, *114*, 49–56.

Atkinson, A., V. Siegel, E. Pakhomov, and P. Rothery (2004), Long-term decline in krill stock and increase in salps within the Southern Ocean, *Nature*, *432*, 100–103.

Brown, L., R. Sanders, G. Savidge, and C. H. Lucas (2003), The uptake of Silica during the spring bloom in the Northeast Atlantic Ocean, *Limnol. Oceanogr.*, *48*(5), 1831–1845.

Buesseler, K., and P. Boyd (2009), Shedding light on processes that control particle export and flux attenuation in the twilight zone of the open ocean, *Limnol. Oceanogr.*, *54*(4), 1210–1232.

Buesseler, K., et al. (2007), Revisiting carbon flux through the ocean's twilight zone, *Science*, *316*, 567–570, doi:10.1126/science.1137959.

Buesseler, K., A. M. P. McDonnell, O. M. E. Schofield, D. Steinberg, and H. Ducklow (2010), High particle export over the continental shelf of the west Antarctic Peninsula, *Geophys. Res. Lett.*, *37*, L22606, doi:10.1029/2010GL045448.

Clarke, A., and L. S. Peck (1991), The physiology of polar marine zooplankton, *Polar Res.*, *10*(2), 355–370.

Ducklow, H. W., M. Erickson, J. Kelly, M. Montes-Hugo, C. A. Ribic, R. C. Smith, S. E. Stammerjohn, and D. M. Karl (2008), Particle export from the upper ocean over the continental shelf of the west Antarctic Peninsula: A long-term record, 1992–2007, *Deep Sea Res., Part II*, *55*(18–19), 2118–2131, doi:10.1016/j.dsr2.2008.04.028.

Dulaiova, H., M. V. Ardelan, P. B. Henderson, and M. A. Charette (2009), Shelf-derived iron inputs drive biological productivity in the southern Drake Passage, *Global Biogeochem. Cycles*, *33*, GB4014, doi:10.1029/2008GB003406.

Eppley, R. W., and B. J. Peterson (1979), Particulate organic matter flux and planktonic new production in the deep ocean, *Nature*, *282*, 677–680, doi:10.1038/282677a0.

Francois, R., S. Honjo, R. Krishfield, and S. Manganini (2002), Factors controlling the flux of organic carbon to the bathypelagic zone of the ocean, *Global Biogeochem. Cycles*, *16*(4), 1087, doi:10.1029/2001GB001722.

Froneman, P. W., E. A. Pakhomov, R. Perissinotto, and V. Meaton (1998), Feeding and predation impact of two chaetognath species *Eukrohnia hamata* and *Sagitta gazellae*m in the vicinity of Marion Island (Southern Ocean), *Mar. Biol.*, *131*, 95–101.

Giering, S. L. C., et al. (2014), Reconciliation of the carbon budget in the ocean's twilight zone, *Nature*, *507*(7493), 480–483, doi:10.1038/nature13123.

González, H. E., and V. Smetacek (1994), The possible role of the cyclopoid copepod Oithonan retarding vertical flux of zooplankton fecal material, *Mar. Ecol. Prog. Ser.*, *113*, 233–246.

Grenfell, T. C., and G. A. Maykut (1977), The optical properties of ice and snow in the Arctic Basin, *J. Glaciol.*, *18*(80), 445–463.

Henson, S. A., R. J. Sanders, and E. Madsen (2012), Global patterns in efficiency of particulate organic carbon export and transfer to the deep ocean, *Global Biogeochem. Cycles*, *26*, GB1028, doi:10.1029/2011GB004099.

Henson, S. A., A. Yoo, and R. Sanders (2014), Variability in efficiency of particulate organic carbon export: A model study, *Global Biogeochem. Cycles*, doi:10.1002/2014GB004965.

Henson, S., R. J. Sanders, E. Madsen, P. Morris, F. Le Moigne, and G. Quartley (2011), A reduced estimate of the strength of the biological carbon pump, *Geophys. Res. Lett.*, *38*, L04066, doi:10.1029/2011GL046735.

Herndl, G., and T. Reinthaler (2013), Microbial control of the dark end of the biological carbon pump, *Nat. Geosci.*, *6*, 718–724, doi:10.1038/ngeo1921.

Heywood, K. J., and B. A. King (2002), Water masses and baroclinic transports in the South Atlantic and Southern Oceans, *J. Mar. Res.*, *60*(5), 639–676.

Iversen, M., and L. K. Poulsen (2007), Coprohexy, coprophagy, and coprochaly in the copepods Calanus helgolandicus, Pseudocalanus elongatus, and Oithona similis, *Mar. Ecol. Prog. Ser.*, *350*, 79–89, doi:10.3354/meps07095.

Kahru, M., B. G. Mitchell, S. T. Gille, C. D. Hewes, and O. Holm-Hansen (2007), Eddies enhance biological production in the Weddell-Scotia Confluence of the Southern Ocean, *Geophys. Res. Lett.*, *34*, L14603, doi:10.1029/2007GL030430.

Kawaguchi K., S. Ishikawa, and O. Matsuda (1986), The overwintering of Antarctic krill (*Euphausia superba* Dana) under the coastal fast ice off the Ongul Islands in Lutzow-Holm Bay, Antarctica, Memoirs of the National Institute of Polar Research 44 (special issue), pp. 67–85.

Korb, R. E., M. Whitehouse, M. Gordon, P. Ward, and A. Poulton (2012), Regional and seasonal differences in microplankton biomass, productivity, and structure across the Scotia Sea: Implications for the export of biogenic carbon, *Deep Sea Res., Part II*, *59-60*, 67–77, doi:10.1016/j.dsr2.2011.06.006.

Kwon, E. Y., F. Primeau, and J. L. Sarmiento (2009), The impact of remineralization on the air-sea carbon balance, *Nat. Geosci.*, *2*, doi:10.1038/NGEO612.

Lam, P., and J. Bishop (2007), High biomass, low export regimes in the Southern Ocean, *Deep Sea Res., Part II*, *54*, 601–638, doi:10.1016/j.dsr2.2007.01.013.

Lam, P., S. Doney, and J. Bishop (2011), The dynamic ocean biological pump: Insights from a global compilation of particulate organic carbon, $CaCO_3$, and opal concentration profiles from the mesopelagic, *Global Biogeochem. Cycles*, *25*, GB3009, doi:10.1029/2010GB003868.

Lancroft, T. M., T. L. Hopkins, J. J. Torres, and J. Donnelly (1991), Oceanic micronektonic/macrozooplanktonic community structure and feeding in ice covered Antarctic waters during the winter (AMERIEZ 1988), *Polar Biol.*, *11*(3), 157–167.

Laws, E., P. Falkowski, W. Smith Jr., H. Ducklow, and J. McCarthy (2000), Temperature effects on export production in the open ocean, *Global Biogeochem. Cycles*, *14*, 1231–1246, doi:10.1029/1999GB001229.

Le Moigne, F. A. C., R. J. Sanders, M. Villa-Alfageme, A. P. Martin, K. Pabortsava, H. Planquette, P. J. Morris, and S. J. Thomalla (2012), On the proportion of ballast versus non-ballast associated carbon export in the surface ocean, *Geophys. Res. Lett.*, *39*, L15610, doi:10.1029/2012GL052980.

Le Moigne, F. A. C., S. Henson, R. J. Sanders, and E. Madsen (2013), Global database of surface ocean particulate organic carbon export fluxes diagnosed from the [234]Th technique, *Earth Syst. Sci. Data Discuss*, *6*, 163–187, doi:10.5194/essd-5-295-2013.

Le Moigne, F. A. C., K. Pabortsava, C. L. J. Marcinko, P. Martin, and R. J. Sanders (2014), Where is mineral ballast important for surface export of particulate organic carbon in the ocean?, *Geophys. Res. Lett.*, doi:10.1002/2014GL061678.

Maiti, K., M. Charette, K. Buesseler, and M. Kahru (2013), An inverse relationship between production and export efficiency in the Southern Ocean, *Geophys. Res. Lett.*, *40*, 1–5, doi:10.1002/grl.50219.

Martin, J. H. (1990), Glacial-interglacial CO_2 change: The iron hypothesis, *Paleoceanography*, *5*(1), 1–13, doi:10.1029/PA005i001p00001.

Martin, J. H., G. Jauner, D. Karl, and W. Broenkow (1987), VERTEX: Carbon cycling in the northeast Pacific, *Deep Sea Res., Part A*, *34*(2), 267–285, doi:10.1016/0198-0149(87)90086-0.

Murphy, E. J., et al. (2013), Comparison of the structure and function of Southern Ocean regional ecosystems: The Antarctic Peninsula and South Georgia, *J. Mar. Syst.*, *109–110*, 22–42, doi:10.1016/j.jmarsys.2012.03.011.

Park, J., I. Oh, H. Kim, and S. Yoo (2010), Variability of SeaWiFS chlorophyll *a* in the southwest Atlantic sector of the Southern Ocean: Strong topographic effects and weak seasonality, *Deep Sea Res., Part I*, *57*(4), 604–620, doi:10.1016/j.dsr.2010.01.004.

Planchon, F., A. J. Cavagna, D. Cardinal, L. Andre, and F. Dehairs (2013), Late summer particulate organic carbon export from mixed layer to mesopelagic twilight zone in Atlantic sector of the Southern Ocean, *Biogeosciences*, *9*, 3423–3477, doi:10.5194/bg-10-803-2013.

Pollard, R. T., et al. (2009), Southern Ocean deep-water carbon export enhanced by natural iron fertilization, *Nature*, *457*, 577–581, doi:10.1038/nature07716.

Poulton, A. J., M. C. Stinchcombe, E. P. Achterberg, D. C. E. Bakker, C. Dumousseaud, H. E. Lawson, G. A. Lee, S. Richier, D. J. Suggett, and J. R. Young (2014), Coccolithophores on the northwest European shelf: Calcification rates and environmental controls, *Biogeosciences*, *11*, 3919–3940, doi:10.5194/bg-11-3919-2014.

Richier, S., E. P. Achterberg, C. Dumousseaud, A. J. Poulton, D. J. Suggett, T. Tyrrell, M. V. Zubkov, and C. M. Moore (2014), Phytoplankton responses and associated carbon cycling during shipboard carbonate chemistry manipulation experiments conducted around northwest European shelf seas, *Biogeosciences*, *11*, 4733–4752, doi:10.5194/bg-11-4733-2014.

Riley, J., R. J. Sanders, C. Marsay, F. Le Moigne, E. Achterberg, and A. Poulton (2012), The relative contribution of fast and slow sinking particles to ocean carbon export, *Global Biogeochem. Cycles*, *26*, GB1026, doi:10.1029/2011GB004085.

Salter, I., R. S. Lampitt, R. Sanders, A. Poulton, A. Kemp, B. Boorman, K. Saw, and R. Pearce (2007), Estimating carbon, silica, and diatom export from a naturally fertilised phytoplankton bloom in the Southern Ocean using PELAGRA: A novel drifting sediment trap, *Deep Sea Res., Part II*, *54*(18–20), 2233–2259, doi:10.1016/j.dsr2.2007.06.008.

Salter, I., A. E. S. Kemp, C. M. Moore, R. S. Lampitt, G. A. Wolff, and J. Holtvoeth (2012), Diatom resting spore ecology drives enhanced carbon export from a naturally iron-fertilized bloom in the Southern Ocean, *Global Biogeochem. Cycles*, *26*, GB1014, doi:10.1029/2010GB003977.

Siegel, V., A. Skibowski, and U. Harm (1992), Community structure of the epipelagic zooplankton community under the sea-ice of the northern Weddell Sea, *Polar Biology*, *12*, 15–24.

Steinberg, D. K., B. Van Mooy, K. Buesseler, P. Boyd, T. Kobari, and D. Karl (2008), Bacterial vs. zooplankton control of sinking particle flux in the ocean's twilight zone, *Limnol. Oceanogr.*, *53*(4), 1327–1338, doi:10.4319/lo.2008.53.4.1327.

Takahashi, T., et al. (2002), Global sea-air CO_2 flux based on climatological surface ocean $p$$CO_2$ and seasonal biological and temperature effects, *Deep Sea Res., Part II*, *49*, 1601–1622, doi:10.1016/S0967-0645(02)00003-6.

Tarling, G. (2013), RRS James Clark Ross Cruise 274, 09 Jan–12 Feb 2013, Sea Surface Ocean Acidification Consortium Cruise to the Southern Ocean, Cambridge, UK, British Antarctic Survey, 220 pp.

Tarling, G. A., R. S. Shreeve, P. Ward, A. Atkinson, and A. G. Hirst (2004), Life-cycle phenotypic composition and mortality of Calanoides acutus (Copepoda: Calanoida) in the Scotia Sea: A modeling approach, *Mar. Ecol. Prog. Ser.*, *272*, 165–181.

Taylor, M. H., M. Losch, and A. Bracher (2013), On the drivers of phytoplankton blooms in the Antarctic marginal ice zone: A modeling approach, *J. Geophys. Res. Oceans*, *118*, 63–75, doi:10.1029/2012JC008418.

Turner, J. (2004), The importance of small planktonic copepods and their roles in pelagic marine food webs, *Zool. Stud.*, *43*(2), 255–266.

Veit, R. R., E. D. Silverman, and I. Everson (1993), Aggregation patterns of pelagic predators and their principal prey, Antarctic Krill, near South Georgia, *J. Anim. Ecol.*, *62*(3), 551–564.

Ward, P., R. Shreeve, M. Whitehouse, B. Korb, A. Atkinson, M. Meredith, D. Pond, J. Watkins, C. Goss, and N. Cunningham (2005), Phyto- and zooplankton community structure and production around South Georgia (Southern Ocean) during summer 2001/02, *Deep Sea Res., Part I*, *52*, 421–441.

Ward, P., A. Atkinson, and G. Tarling (2012a), Mesozooplankton community structure and variability in the Scotia Sea: A seasonal comparison, *Deep Sea Res., Part II*, *59*, 78–92, doi:10.1016/j.dsr2.2011.07.004.

Ward, P., et al. (2012b), Food web structure and bioregions in the Scotia Sea: A seasonal synthesis, *Deep Sea Res., Part II*, *59*, 253–266.

Wilson, S. E., D. Steinberg, and K. Buesseler (2008), Changes in fecal pellet characteristics with depth as indicators of zooplankton repackaging of particles in the mesopelagic zone of the subtropical and subarctic North Pacific ocean, *Deep Sea Res., Part II*, *55*, 1636–1647, doi:10.1016/j.dsr2.2008.04.019.

Wishner, K. F., C. Gelfan, M. Gowing, D. Outram, M. Rapien, and R. Williams (2008), Vertical zonation and distributions of calanoid copepods through the low oxycline of the Arabian Sea oxygen minimum zone, *Prog. Oceanogr.*, *78*(2), 163–191, doi:10.1016/j.pocean.2008.03.001.